Distance Metrology with Integrated Mode-Locked Ring Laser

Hei, Kefei; Shi, Guang; Hansel, Andreas; Deng, Zhongwen; Latkowski, Sylwester; Van Den Berg, Steven A.; Bente, Erwin; Bhattacharya, Nandini

DOI
10.1109/JPHOT.2019.2940068

Publication date
2019

Document Version
Final published version

Published in
IEEE Photonics Journal

IEEE Photonics Journal
An IEEE Photonics Society Publication

Open Access

Distance Metrology With Integrated Mode-Locked Ring Laser

Volume 11, Number 6, December 2019

Kefei Hei
Guang Shi
Andreas Hänsel
Zhongwen Deng
Sylwester Latkowski
Steven A. Van den Berg
Erwin Bente
Nandini Bhattacharya

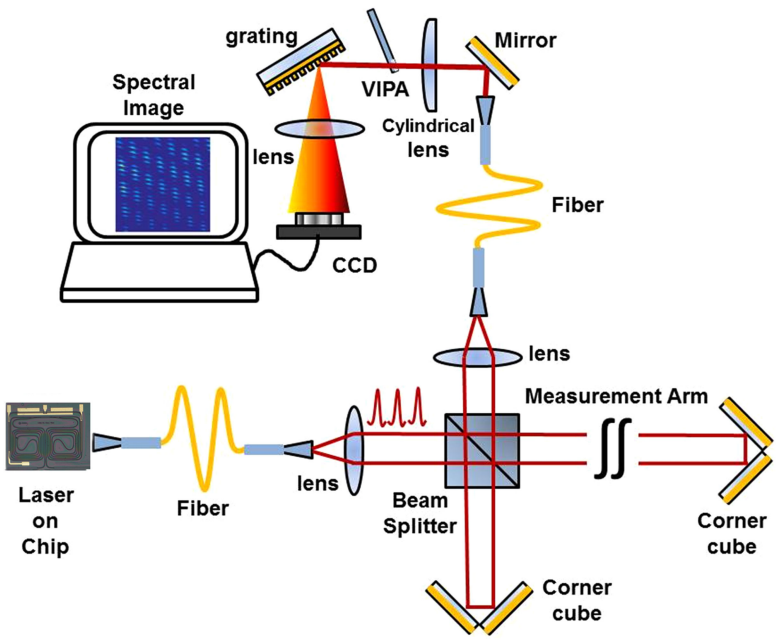

DOI: 10.1109/JPHOT.2019.2940068

IEEE photonics SOCIETY
IEEE

Distance Metrology With Integrated Mode-Locked Ring Laser

Kefei Hei,[1] **Guang Shi**,[2] **Andreas Hänsel**,[1] **Zhongwen Deng**,[1,5] **Sylwester Latkowski**,[3] **Steven A. Van den Berg**,[4] **Erwin Bente**,[3] **and Nandini Bhattacharya**[1]

[1]Optics Research Group, Delft University of Technology, 2628 CJ Delft, The Netherlands
[2]School of Mechanical Engineering, Hangzhou Dianzi University, Hangzhou 310018, China
[3]Institute for Photonic Integration, Eindhoven University of Technology, 5612 AP Eindhoven, The Netherlands
[4]National Metrology Institute VSL, 2629 JA Delft, The Netherlands
[5]State Key Laboratory for Manufacturing Systems Engineering, Xian Jiaotong University, Xian 710054, China

DOI:10.1109/JPHOT.2019.2940068

Manuscript received April 26, 2019; revised August 12, 2019; accepted September 3, 2019. Date of publication September 9, 2019; date of current version October 31, 2019. This work was supported by the European Metrology Research Program (EMRP), Project SIB60 Surveying and the Dutch Ministry of Economic Affairs. The EMRP is jointly funded by the EMRP participating countries within EURAMET and the European Union. The work of K. Hei and Z. Deng was supported by China Scholarship Council (CSC) grants. Corresponding author: Kefei Hei (e-mail: K.Hei@tudelft.nl).

Abstract: The measurement of distance plays an integral part in many aspects of modern societies. In this paper an integrated mode-locked laser on a chip is used for distance measurement based on mode-resolved interferometry. The emission from the on-chip source with a repetition rate of 2.5 GHz and a spectral bandwidth of 3 nm is coupled into a Michelson interferometer. The interferometer output is recorded as a spectral interferogram, which is captured in a single camera image. The images are analyzed using Hilbert transform to extract the distance. The distance derived shows a deviation of 6 μm from the reference, for a distance up to 25 mm. We also demonstrate interferometry with repetition frequency sweep which can also be used with the source. Performance is expected to be better in the near future with the rapid developments in the field of on-chip laser sources which are demonstrating larger spectral widths and coherence lengths.

Index Terms: Metrology, mode-locked lasers and integrated optics.

1. Introduction

Dimensional metrology has found applications in many areas of modern life. Applications ranging from geodetic monitoring, environmental monitoring and formation flight for interferometry in space to precision engineering require measurements of length or displacement. Laser based interferometric techniques are advancing rapidly due to the new laser sources, advances in detector technology, electronics and computational devices. Pulsed laser sources, which are extremely stable, like the frequency comb, have also led to techniques, which measure larger distances with extremely high accuracies [1]–[3]. In most cases the experiments that demonstrate these techniques consist of large setups on experimental tables. Applications require devices which can implement dimensional metrology but have a small footprint in terms of size, power consumption

and lower cost. These devices could then be used universally to control processes in industry, remote environmental monitoring or flown in satellites.

The development of mode-locked laser sources has been the main instigator of the major leaps made in the field of distance metrology [1]. Significant improvements have been made towards stabilizing mode-locked lasers to an unprecedented level, leading to frequency comb lasers [4]. Optical frequency combs with their extreme stability have found a multitude of applications since their emergence at the beginning of this century [5]. While the goal of the initial applications was to provide an optical frequency standard, the versatility and reliability of frequency combs sparked new research in high-resolution optical spectroscopy and length metrology [6]. Distance metrology has been implemented using methods where the frequency comb is used to reference continuous wave lasers [7]–[10], as a source for time-of-flight measurement [11] and for the multiplication effect by tuning the repetition frequency f_{rep} [12]. Other applications in spectroscopy and length metrology make use of the strict definition of the optical spectrum, which is directly related to a frequency standard, to extract distance and spectral information from the interferogram of the many individual comb modes. Several techniques based on this method have been successfully demonstrated for distance measurement. These include inter-pulse cross correlation interferometry [13]–[15], dispersive interferometry [16], [17],spectral interferometry [2], [18] and dual comb multi-heterodyne interferometry [3], [19], [20] which directly use the spectral properties of the frequency comb to extract the distance being measured. Spectral interferometry method is one of the most accurate methods, of which the relative accuracies remain in the 10^{-7}–10^{-8} range mainly due to the uncertainty of the refractive index and are not limited by the performance of the frequency comb.

For the technology to become more accessible for industrial and outdoor measurements, integrating the laser source [21] is desirable. The Ti:Sapphire oscillator based frequency combs are extremely accurate but not so practical for measurements where portable setups or compact devices are required. Fiber-based frequency comb laser sources are portable though the long optical path length in the oscillator results in very low repetition rate, in the order of hundreds of MHz. Since the repetition rate corresponds to the comb mode spacing in the frequency domain, a higher repetition rate, in the order of GHz, loosens the resolution requirements of the spectrometer for spectrometer based measurements. External cavities can be employed to filter some of the comb modes until individual modes can be resolved, but increase the complexity of the system and are sensitive to vibrations [22]. An integrated mode-locked laser on a chip with a high repetition rate can be the key device which can move this technology from laboratories to industrial and outdoor applications. Ideally this device should have a small footprint in size and power consumption. Additionally this device should be sufficiently isolated so that it remains stable in spite of variations in its ambient environment.

In this work we present a distance measurement based on mode-resolved interferometry [18] with a monolithically integrated mode-locked laser [23]. This laser features a repetition rate of 2.5 GHz, which ensures that the modes can be separated by most VIPA (Virtually Imaged Phased Array) spectrometers. Compared to other spectral interferometry methods [18], [24], the phase calculation method with Hilbert transform can extract phase directly and accurately, which can improve fitting results. The performance of distance measurement and repetition frequency tuning are also shown.

2. Measurement Principles

The measurement method is based on a Michelson interferometry. As an input the light from a mode-locked chip laser is used, containing about 120 modes. The laser beam is split into two arms, a reference arm and a measurement arm, and recombined again. Then the combined beam is spectrally resolved by a VIPA spectrometer. The intensity of each mode changes periodically with wavelength. The interference intensity can be written as:

$$I(\phi) = I_0 \cos\phi, \quad \phi = \frac{4\pi L n}{\lambda} \tag{1}$$

with I_0 the intensity of the light sent into the interferometer, L, the path length difference of the interferometer arms (single path), λ the vacuum wavelength and n the air refractive index. The phase can be written as :

$$\phi = \frac{4\pi L f n}{c}, \tag{2}$$

with f the optical frequency and c the speed of light in vacuum. The derivative of phase with respect to frequency can be written as:

$$\frac{d\phi}{df} = \frac{4\pi L}{c}\left(n + f\frac{dn}{df}\right) = \frac{4\pi L}{c} n_g, \tag{3}$$

with n_g the group refractive index:

$$n_g = n - \lambda\frac{dn}{d\lambda} = n + f\frac{dn}{df}. \tag{4}$$

The distance can be written as:

$$L = \frac{d\phi}{df}\frac{c}{4\pi n_g}. \tag{5}$$

We define L_{pp} as the pulse-to-pulse distance in the medium, which is written as:

$$L_{pp} = \frac{c}{f_{\text{rep}} n_g}, \tag{6}$$

with f_{rep} is the repetition frequency of frequency comb. The phase of each mode is obtained by Hilbert transform. If the distance is less than $\frac{1}{4}L_{pp}$, there is no ambiguity to unwrap the phase. Then linear fit is used to obtain the the phase change with frequency. The linear fit result is $\phi = K \cdot p + b$. This implies that the refractive index changes linearly with wavelength. Here K and b are fitting parameters and p is a label which is relative to a specific mode as defined by $f_p = f_{\text{rep}}(Q + p) + f_0$, where Q is a very large integer. With $d\phi/df = K/f_{\text{rep}}$, this leads to

$$L = \frac{K}{f_{\text{rep}}}\frac{c}{4\pi n_g}. \tag{7}$$

If the distance being measured is between $\frac{1}{4}L_{pp}$ and $\frac{1}{2}L_{pp}$, K is negative and L can be written as:

$$L = \frac{2\pi + K}{f_{\text{rep}}}\frac{c}{4\pi n_g}. \tag{8}$$

Just a linear fit is not enough to determine K, because the sign of K is unknown. It is possible to determine K with several methods, such as changing the f_{rep}, which will be shown in the following section.

Within $\frac{1}{2}L_{pp}$ the distance L is defined with non-ambiguity. When L is larger than $\frac{1}{2}L_{pp}$, the interference patterns are repeating for each $\frac{1}{2}L_{pp}$, because the phase change is more than 2π if $L > \frac{1}{2}L_{pp}$. Using the linear fit, we can only obtain phase change which is less than 2π. The arbitrary distance can be written as:

$$L_t = \frac{1}{2}mL_{pp} + L, \tag{9}$$

where m is an integer and can also be determined by sweeping the f_{rep}.

3. Experimental Setup

The setup for the experiment presented in this work has three main components: the monolithically integrated mode-locked laser, the Michelson interferometer with reference and measurement arm, and the VIPA spectrometer. Optical single-mode fibers are used to transfer the light between those

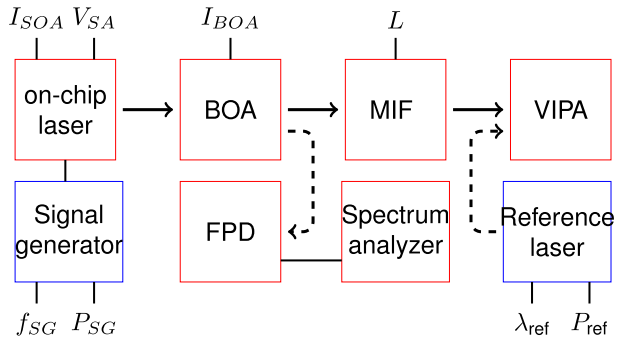

Fig. 1. The schematic diagram of the experimental setup showing the different parts. Light is collected with a lensed fiber from the on-chip laser and amplified in the booster optical amplifier (BOA). The amplified light is sent to the Michelson interferometer (MIF) with reference and measurement arm. A VIPA spectrometer (VIPA) records interferograms from which the length of the measurement arm can be extracted. A fast photo-detector (FPD) in combination with an electronic spectrum analyzer allowed for measuring the repetition rate of the laser. The light is guided with single-mode fibers between the different parts of the setup. A signal generator was used for hybrid mode-locking.

components. A schematic of the setup is shown in Fig. 1. The different segments and their control parameters are explained in the following sections.

3.1 Monolithically Integrated Laser

A monolithically integrated mode-locked laser, with a repetition rate of $f_{\text{rep}} \approx 2.5$ GHz at a wavelength of 1.58 μm, was realized on the InP-based multi-project wafer run by SMART Photonics [25]. The laser features a 33 mm long cavity ring. Phase-control elements, gain sections and saturable absorbers in the cavity allow for tuning and optimization of the laser output. The chip was mounted on an aluminum sub-carrier and the electrical contacts wire-bonded to a printed circuit board, which allowed for easier electrical access for controlling the laser. The laser was operated at room temperature without any active cooling or temperature stabilization. The mode-locking of the laser could be achieved either by passive means or by using hybrid mode-locking. Passive mode-locking was realized applying DC (direct current) bias to the saturable absorber and the gain segments. In the case of hybrid mode-locking an additional RF (radio frequency) signal was fed to the absorber via a bias tee, which matched the f_{rep} of the chip in passive mode-locking operation. In hybrid mode-locking f_{rep} could be pinned to a fixed value over the course of the entire experiment, while in a passively locked operation the repetition rate of the laser experienced drift. The current control of the laser was driven by a Thorlabs LDC8005 in a PRO8000 chassis. The saturable absorber was controlled with a National Instruments NI9923 in cDAQ-9178 chassis. The RF signal was provided by a Rohde & Schwarz SMB100 A signal generator. The chip featured angled output ports with anti-reflective coatings, from which the light was collected with a tapered fiber (OZ-optics TSMJ-EA-1550-9/125-0.25-7-2.5-14-1-AR). In this experiment the light from the mode-locked laser was amplified through a booster optical amplifier (BOA) S9FC1004P by Thorlabs, which is a semiconductor based amplifier. An APC circulator, Thorlabs 6015-3, was placed before the BOA to prevent light from the BOA from entering the chip and disturbing the laser operation. The repetition frequency of the laser was measured with a fast photo-detector (Newport 818-BB-35F) in combination with a RIGOL DSA1030 spectrum analyzer. For hybrid mode locking the signal generator provided an RF signal with matching frequency $f_{SG} = f_{\text{rep}}$ and an output power of $P_{SG} = 10$ dBm. A typical mode-resolved spectrum recorded by VIPA spectrometer has been shown in Fig. 2. The intensity of each mode is modulated by VIPA and this modulation can be canceled by the normalization. The further details of the pulsed laser on a chip have already been reported by Latkowski [23].

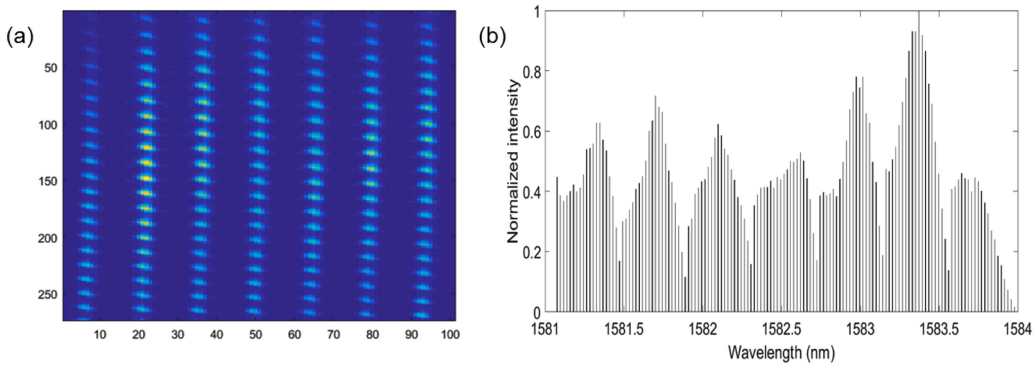

Fig. 2. (a) The two-dimensional VIPA image as recorded by the camera containing the spectral information. (b) VIPA modulated spectrum obtained from the image shown in (a).

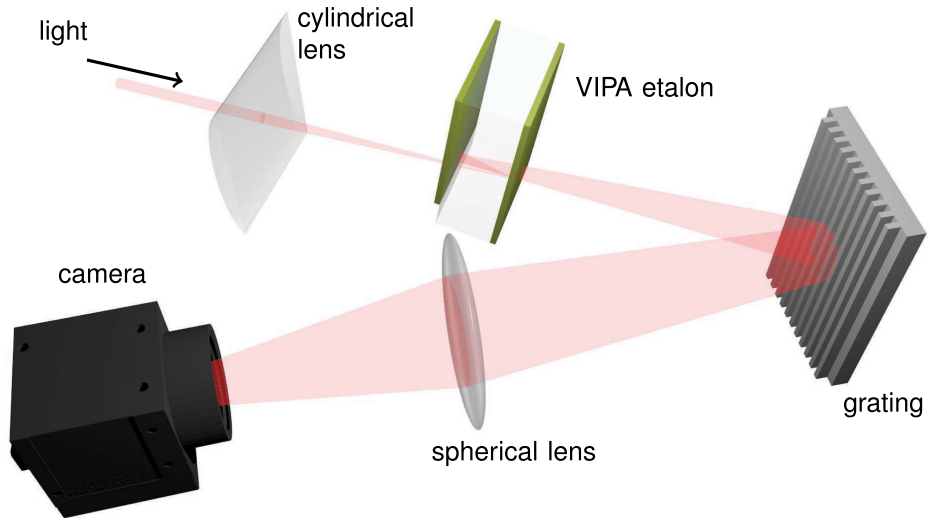

Fig. 3. A schematic of the VIPA spectrometer. Light is focused using a cylindrical lens on the VIPA etalon which then disperses the light spectrally in the y-direction. A grating is used as a post-disperser in the x-direction to separate the different orders. The angularly dispersed frequency information is then converted to position information on a camera.

3.2 Michelson Interferometer

One of the key components for the distance measurement setup is the Michelson interferometer. The path length difference between the known reference arm and variable measurement arm results in an interferogram on the VIPA spectrometer. For the short distance measurement, measurement arm was varied using the translation stage M-112.1DG from PI with a total movement range of 25 mm. A PI C-863 DC motion controller was used to drive the translation stage. For the long distance measurement, the measurement arm has a maximum length of 1.5 m and consists of a long rail with electric carriage.

3.3 VIPA Spectrometer

The virtually imaged phased array spectrometer consists of several components, which are shown in Fig. 3. In the spectrometer the combination of cylindrical lens and VIPA etalon results in wavelength-dependent transmission for different angles and thus acts as an angular disperser. The VIPA etalon from Precision Photonics (S-LAA71) consists of a 1.75 mm thick glass plate. The front side of the

etalon is covered with a highly reflective coating with a reflectance of 99.5%, except of a small window, which is left uncoated to allow the beam to enter the etalon. The output side's coating provided a reflectance of 96%. A small angle between the etalon and the incoming beam allows for several reflections within the etalon. The transmission can be explained with the creation of an array of virtual light sources, which can constructively interfere if angle and wavelength are matched [26], [27], thus causing angular dispersion in the vertical plane. The VIPA etalon has a high resolution, but a low free spectral range (FSR), so the spectral orders overlap, therefore a grating, Spectrogon UK (G1100 31x50x10 NIR, 1100 lines/mm), in orthogonal orientation is used as a post-disperser, creating dispersion in the horizontal plane. The angularly dispersed beam is then focused onto different positions on the detector plane of the camera, by a lens, where each position corresponds to an optical frequency. A continuous broadband light source would create a vertical line pattern on the infra-red camera, XenICs (XEVA-FPA-1.7-640). If the spectrometer allows for a separation of the individual laser modes, a point pattern will be visible, as shown in references [2], [22]. The spectral data is extracted by relating the position on the camera plane to its corresponding frequency. This is done by following the lines or the lines of dots on the camera image. When following one line, spectral data for the span of one FSR of the VIPA can be obtained. To exceed this wavelength range, neighboring lines have to be read out in the same fashion, which allows for stitching of the complete spectra out of the contributions of the individual lines of the camera image [2], [22]. In this experiment the VIPA spectrometer had a resolution of 680 MHz with an FSR of 50 GHz for a single line. The modes of the laser, which are spaced by 2.5 GHz, are spectrally resolved by the VIPA spectrometer. The VIPA spectrometer was calibrated with an Agilent 6015-3-APC tunable single-mode laser in an 8163B mainframe, which allowed for identifying the FSR and also provided the wavelength calibration. This calibration is only used to get the correct stitching of the spectra.

4. Results and Discussion

In order to test the ability of distance measurement with the integrated mode-locked ring laser, we measured a short distance using a high accuracy translation stage and a long distance which were measured simultaneously with the laser and counting HeNe interferometer for comparison. We also swept the repetition frequency to see the change in the fringes. The results will be shown in the following sections.

4.1 Repetition Frequency Sweep for Determination of K

The technique used to extract the distance reported in this paper requires knowledge of the sign of fitting parameter K. One method to solve this problem is to change the f_{rep}. When the laser is hybrid mode locked, f_{rep} is much easier to change. Fig. 4 shows the fitting results with different repetition frequency. The relation between K and f_{rep} is almost linear and allows the determination of the sign of K. This is especially significant for absolute distance measurement for a long distance. From the particular example Fig. 4, it is found that K is positive.

4.2 Distance Measurement for Short Distance

The distance measurements were performed with a high accuracy translation stage which has a unidirectional repeatability of 0.1 μm. Initially the carriage was positioned at the beginning of the stage and the images of the initial position were recorded. Then the carriage was moved in 5 mm increments, and images were taken. At every position, five measurements were recorded. The environment conditions were well controlled in the clean room. A typical phase measurement and unwrapped phase with a linear fit are shown in Fig. 5. Each sample on the horizontal axis corresponds to a wavelength of the frequency comb.

The optical distance measurement is compared with the value given by the translation stage. Fig. 6 shows the outcome of this analysis. When averaged over five measurements the integrated

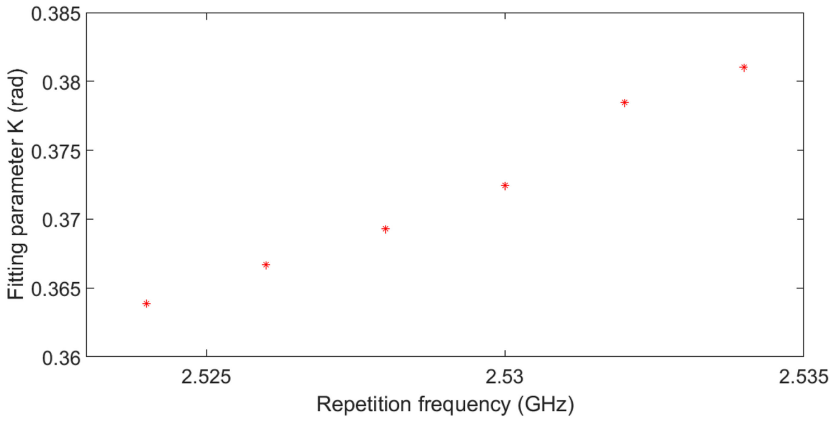

Fig. 4. The fitting results for different repetition frequency. The repetition frequency is changed from 2.524 to 2.534 GHz in 2 MHz increments.

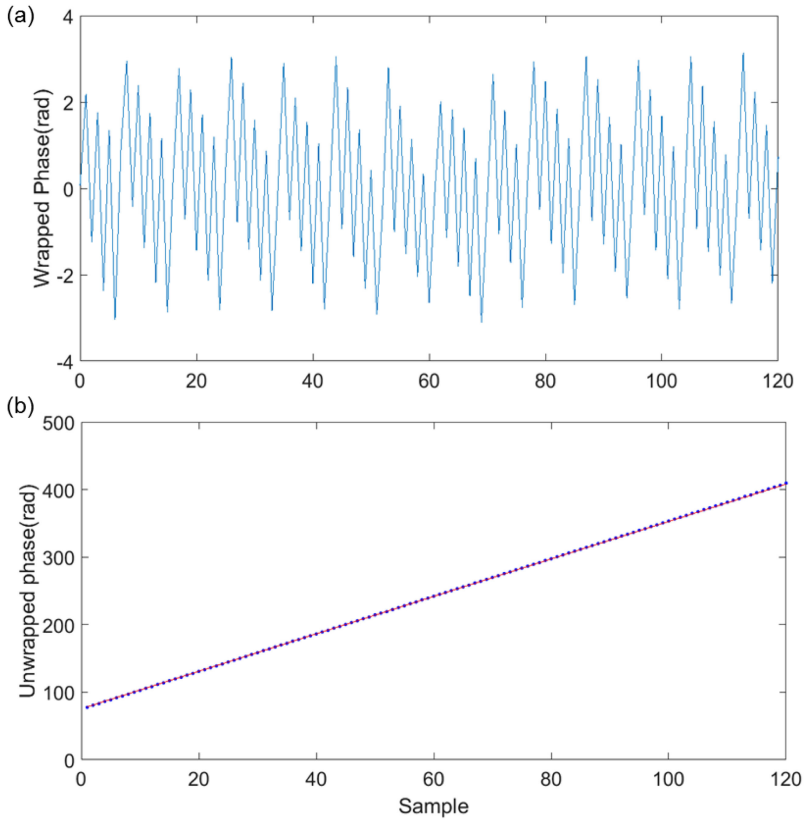

Fig. 5. Typical phase measurements and fitting result. (a) The wrapped phase obtained by Hilbert transform for 120 modes. (b) The unwrapped phase - blue points and linear fit - red line.

comb laser and the length given by the translation stage agree within 6 μm with a standard deviation of 1.4 μm.

The linear fitting uncertainty is less than 5×10^{-4}, which corresponds to 12.5 μm. This is the main contribution to the distance measurement uncertainty, which is much larger than the group refractive index and environmental effects. This error is mostly arising from the limited number

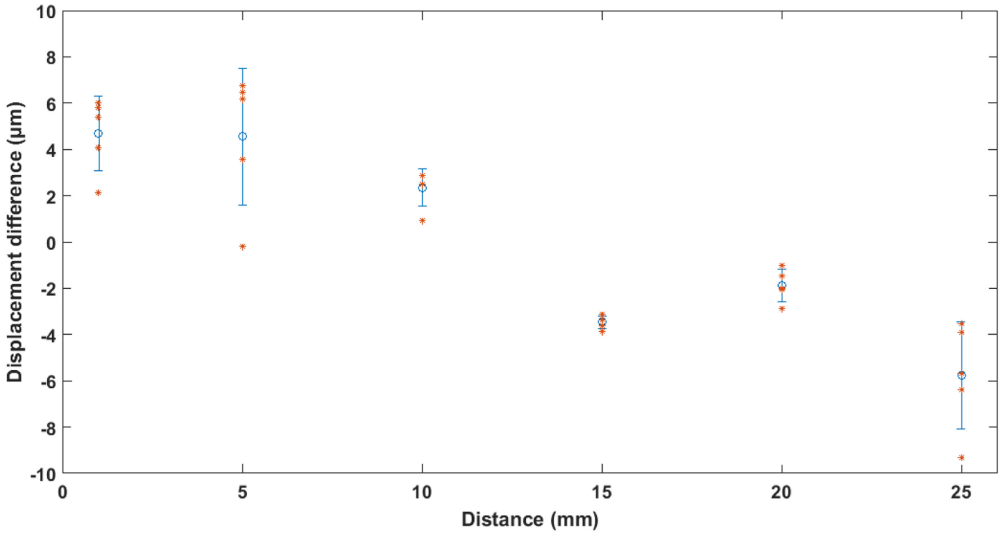

Fig. 6. The displacement differences between distance measurements with a integrated comb laser and length given by the translation stage for distances up to 25 mm. The error bars show the standard deviation of the measurements.

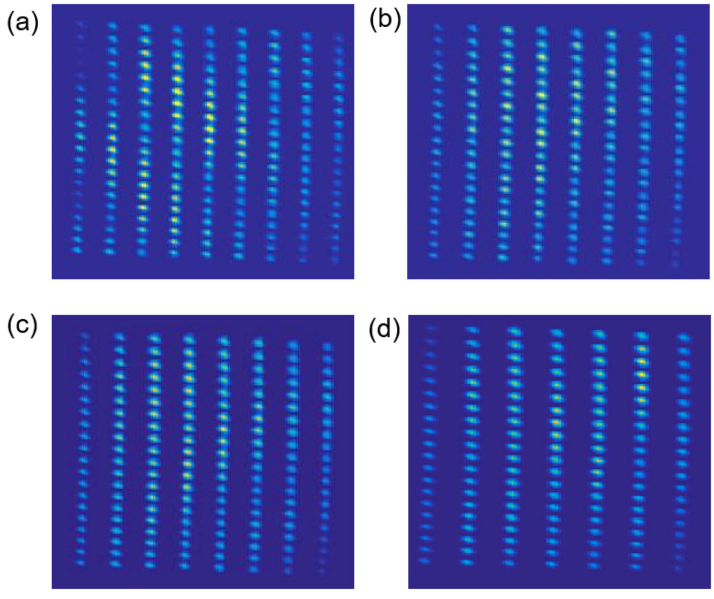

Fig. 7. VIPA images of the interference for different displacements. The arm length differences for the images are (a) $L = 0.7$ cm, (b) $L = 19$ cm, (c) $L = 40$ cm, and (d) $L = 70$ cm.

of modes available from the laser. Several simple improvements will enhance the accuracy of a device based on this experiment. For the chip used in this work the spectral bandwidth is 3 nm (120 modes) in comparison to the measurement with several thousands of modes reported by Van den Berg [18] using a Ti:Sapphire laser. New mode-locked laser designs already extend the bandwidth to 40 nm [23], [28], so this will not be a bottleneck in taking the technology further. Another easy improvement can be increasing the repetition frequency. As shown in [24], with a laser of tens of gigahertz repetition frequency a highly accurate result can be also obtained.

4.3 Distance Measurement for Long Distance

A distance up to 70 cm was also measured with chip laser. The setup is similar to short distance measurement, except a 1.5 m bench was used to replace the translation stage. The displacement of the bench could not be directly read out, therefore a counting HeNe interferometer was used for comparison. However, the results of long distance measurements were much worse than short distance measurement. The integrated comb laser and counting HeNe interferometer measurements agree within 5 mm over a distance of 70 cm. Though as mentioned in [18], the method does not need the offset frequency f_0 to be locked, it only works when the distance is less than $\frac{1}{2}L_{pp}$. If the distance is longer than $\frac{1}{2}L_{pp}$, the interference occurs between different pulses. The interference signal changing with distance is shown in Fig. 7. The interference fringes at the distance of 0.7 cm can be clearly seen but for a distance of 70 cm the fringes almost disappear. The pulses at different moment are not stable in frequency and the interference is not stable enough to be recorded. The interference signal is not DC anymore. The integration time of camera is 10 ms, which means that the image is obtained by averaging 2.5×10^7 pulses. The averaging reduces the interference signal and increases the uncertainty of fitting result. A new laser has been published with a 12-nm 10-dB output optical spectrum and a narrow longitudinal mode linewidth ($<$400 kHz) [29]. This new laser can dramatically improve the measurement range at these distances.

5. Conclusion

We have shown that mode-resolved spectral interferometry with an on-chip laser is possible. This is promising for frequency comb-based distance measurement, since miniaturization allows for potentially huge cost reduction, reduction of energy consumption and footprint, which could enable a wide range of applications for which current frequency comb systems are too bulky and expensive. A tunable mode-locked laser can easily solve the ambiguity problem of spectral interferometry method by varying the repetition frequency, which is significant for absolute long distance measurement. However, further improvement on spectral width and coherence length will be needed to reach the results obtained with traditional frequency comb sources. Given the rapid developments in the field, though, competing performance may be demonstrated in near future. Several improvements of lasers like larger bandwidth [23], [28] and narrow linewidth [29] have been reported, which will further enhance the stability of the on-chip laser and improve the measurement accuracy for a wide range of applications.

References

[1] K. Minoshima and H. Matsumoto, "High-accuracy measurement of 240-m distance in an optical tunnel by use of a compact femtosecond laser," *Appl. Opt.*, vol. 39, no. 30, pp. 5512–5517, 2000.
[2] S. A. Van den Berg, S. T. Persijn, G. J. P. Kok, M. G. Zeitouny, and N. Bhattacharya, "Many-wavelength interferometry with thousands of lasers for absolute distance measurement," *Phys. Rev. Lett.*, vol. 108, no. 18, 2012, Art. no. 183901.
[3] I. Coddington, W. C. Swann, L. Nenadovic, and N. R. Newbury, "Rapid and precise absolute distance measurements at long range," *Nature Photon.*, vol. 3, no. 7, pp. 351–356, 2009.
[4] J. L. Hall, "Optical frequency measurement: 40 years of technology revolutions," *IEEE J. Sel. Topics Quantum Electron.*, vol. 6, no. 6, pp. 1136–1144, Nov./Dec. 2000.
[5] S. A. Diddams, "The evolving optical frequency comb [invited]," *J. Opt. Soc. Amer. B*, vol. 27, no. 11, pp. B51–B62, 2010.
[6] N. R. Newbury, "Searching for applications with a fine-tooth comb," *Nature Photon.*, vol. 5, no. 4, pp. 186–188, 2011.
[7] T. Yoon, J. Ye, J. L. Hall, and J.-M. Chartier, "Absolute frequency measurement of the iodine-stabilized he-ne laser at 633 nm," *Appl. Phys. B*, vol. 72, no. 2, pp. 221–226, 2001.
[8] Y. Salvadé, N. Schuhler, S. Lévêque, and S. Le Floch, "High-accuracy absolute distance measurement using frequency comb referenced multiwavelength source," *Appl. Opt.*, vol. 47, no. 14, pp. 2715–2720, 2008.
[9] S. Hyun, M. Choi, B. J. Chun, S. Kim, S.-W. Kim, and Y.-J. Kim, "Frequency-comb-referenced multi-wavelength profilometry for largely stepped surfaces," *Opt. Exp.*, vol. 21, no. 8, pp. 9780–9791, 2013.
[10] E. Baumann, F. R. Giorgetta, J.-D. Deschênes, W. C. Swann, I. Coddington, and N. R. Newbury, "Comb-calibrated laser ranging for three-dimensional surface profiling with micrometer-level precision at a distance," *Opt. Exp.*, vol. 22, no. 21, pp. 24 914–24 928, 2014.
[11] J. Lee, Y.-J. Kim, K. Lee, S. Lee, and S.-W. Kim, "Time-of-flight measurement with femtosecond light pulses," *Nature Photon.*, vol. 4, no. 10, pp. 716–720, 2010.

[12] Y. Nakajima and K. Minoshima, "Highly stabilized optical frequency comb interferometer with a long fiber-based reference path towards arbitrary distance measurement," *Opt. Exp.*, vol. 23, no. 20, pp. 25 979–25 987, 2015.
[13] J. Ye, "Absolute measurement of a long, arbitrary distance to less than an optical fringe," *Opt. Lett.*, vol. 29, no. 10, pp. 1153–1155, 2004.
[14] M. Cui, M. G. Zeitouny, N. Bhattacharya, S. A. Van den Berg, H. P. Urbach, and J. J. M. Braat, "High-accuracy long-distance measurements in air with a frequency comb laser," *Opt. Lett.*, vol. 34, no. 13, pp. 1982–1984, 2009.
[15] P. Balling, P. Křen, P. Mašika, and S. Van den Berg, "Femtosecond frequency comb based distance measurement in air," *Opt. Exp.*, vol. 17, no. 11, pp. 9300–9313, 2009.
[16] K.-N. Joo, Y. Kim, and S.-W. Kim, "Distance measurements by combined method based on a femtosecond pulse laser," *Opt. Exp.*, vol. 16, no. 24, pp. 19 799–19 806, 2008.
[17] M. Cui, M. G. Zeitouny, N. Bhattacharya, S. A. Van den Berg, and H. P. Urbach, "Long distance measurement with femtosecond pulses using a dispersive interferometer," *Opt. Exp.*, vol. 19, no. 7, pp. 6549–6562, 2011.
[18] S. A. Van den Berg, S. Van Eldik, and N. Bhattacharya, "Mode-resolved frequency comb interferometry for high-accuracy long distance measurement," *Sci. Rep.*, vol. 5, 2015, Art. no. 14661.
[19] T.-A. Liu, N. Newbury, and I. Coddington, "Sub-micron absolute distance measurements in sub-millisecond times with dual free-running femtosecond Er fiber-lasers," *Opt. Exp.*, vol. 19, no. 19, pp. 18 501–18 509, 2011.
[20] R. Yang, F. Pollinger, K. Meiners-Hagen, M. Krystek, J. Tan, and H. Bosse, "Absolute distance measurement by dual-comb interferometry with multi-channel digital lock-in phase detection," *Meas. Sci. Technol.*, vol. 26, no. 8, 2015, Art. no. 084001.
[21] L. C. Sinclair *et al.*, "Operation of an optically coherent frequency comb outside the metrology lab," *Opt. Exp.*, vol. 22, no. 6, pp. 6996–7006, 2014.
[22] R. Šmíd, A. Hänsel, L. Pravdová, J. Sobota, O. Číp, and N. Bhattacharya, "Comb mode filtering silver mirror cavity for spectroscopic distance measurement," *Rev. Sci. Instrum.*, vol. 87, no. 9, 2016, Art. no. 093107.
[23] S. Latkowski *et al.*, "Monolithically integrated 2.5 GHz extended cavity mode-locked ring laser with intracavity phase modulators," *Opt. Lett.*, vol. 40, no. 1, pp. 77–80, 2015.
[24] A. Lešundák, D. Voigt, O. Cip, and S. van den Berg, "High-accuracy long distance measurements with a mode-filtered frequency comb," *Opt. Exp.*, vol. 25, no. 26, pp. 32 570–32 580, 2017.
[25] SMART Photonics B.V. [Online]. Available: http://www.smartphotonics.nl
[26] A. Vega, A. M. Weiner, and C. Lin, "Generalized grating equation for virtually-imaged phased-array spectral dispersers," *Appl. Opt.*, vol. 42, no. 20, pp. 4152–4155, 2003.
[27] S. Xiao and A. Weiner, "2-D wavelength demultiplexer with potential for $\geq$ 1000 channels in the c-band," *Opt. Exp.*, vol. 12, no. 13, pp. 2895–2902, Jun. 2004.
[28] V. Moskalenko, J. Koelemeij, K. Williams, and E. Bente, "Study of extra wide coherent optical combs generated by a QW-based integrated passively mode-locked ring laser," *Opt. Lett.*, vol. 42, no. 7, pp. 1428–1431, 2017.
[29] Z. Wang *et al.*, "A III-V-on-Si ultra-dense comb laser," *Light, Sci. Appl.*, vol. 5, no. 5, 2017, Art. no. e16260.